# Quantifying the Attenuation of the Ketamine Pharmacological Magnetic Resonance Imaging Response in Humans: A Validation Using Antipsychotic and Glutamatergic Agents[S]

O. M. Doyle, S. De Simoni, A. J. Schwarz, C. Brittain, O. G. O'Daly, S. C. R. Williams, and M. A. Mehta

*King's College London, Department of Neuroimaging, Institute of Psychiatry, London, United Kingdom (O.M.D., S.D.S., O.G.O'D., S.C.R.W., M.A.M.); Translational Medicine, Eli Lilly and Company, Indianapolis, Indiana (A.J.S.); Department of Psychological and Brain Sciences, Indiana University, Bloomington, Indiana (A.J.S.); and Statistics, Eli Lilly and Company, Surrey, United Kingdom (C.B.)*

## ABSTRACT

Ketamine acts as an *N*-methyl-D-aspartate receptor antagonist and evokes psychotomimetic symptoms resembling schizophrenia in healthy humans. Imaging markers of acute ketamine challenge have the potential to provide a powerful assay of novel therapies for psychiatric illness, although to date this assay has not been fully validated in humans. Pharmacological magnetic resonance imaging (phMRI) was conducted in a randomized, placebo-controlled crossover design in healthy volunteers. The study comprised a control and three ketamine infusion sessions, two of which included pretreatment with lamotrigine or risperidone, compounds hypothesized to reduce ketamine-induced glutamate release. The modulation of the ketamine phMRI response was investigated using univariate analysis of prespecified regions and a novel application of multivariate analysis across the whole-brain response. Lamotrigine and risperidone resulted in widespread attenuation of the ketamine-induced increases in signal, including the frontal and thalamic regions. A contrasting effect across both pretreatments was observed only in the subgenual prefrontal cortex, in which ketamine produced a reduction in signal. Multivariate techniques proved successful in both classifying ketamine from placebo (100%) and identifying the probability of scans belonging to the ketamine class (ketamine pretreated with placebo: 0.89). Following pretreatment, these predictive probabilities were reduced to 0.58 and 0.49 for lamotrigine and risperidone, respectively. We have provided clear demonstration of a ketamine phMRI response and its attenuation with both lamotrigine and risperidone. The analytical methodology used could be readily applied to investigate the mechanistic action of novel compounds relevant for psychiatric disorders such as schizophrenia and depression.

## Introduction

*N*-Methyl-D-aspartate (NMDA) antagonists induce symptoms resembling schizophrenia in healthy humans, supporting their use as a model to study the role of the glutamate system in psychoses (Farber et al., 1995; Duncan et al., 2000).

Ketamine, in particular, has been widely used to investigate the role of glutamatergic dysfunction in humans, with acute challenge at subanesthetic doses inducing positive and negative symptoms and impairing cognition (Krystal et al., 1994; Morgan et al., 2004). Across different species and modalities, neuroimaging markers also show robust ketamine-induced changes (Vollenweider et al., 1997; Duncan et al., 1998b; Langsjo et al., 2004; Deakin et al., 2008; Chin et al., 2011; Stone et al., 2012; De Simoni et al., 2013).

Imaging markers of acute ketamine challenge are sensitive to modulation by pretreatment with antipsychotics and compounds that reduce glutamate transmission. In animals, the antipsychotics clozapine and olanzapine, the anticonvulsant lamotrigine, and metabotropic glutamate 2/3 receptor agonists or potentiators all attenuate the effects of ketamine or another NMDA antagonist, phencyclidine (PCP), on markers of brain activity (Duncan et al., 1998a, 2000; Lorrain et al.,

**ABBREVIATIONS:** AUC, area under the curve; BOLD, blood oxygen level dependent; g-map, multivariate map; GPC, Gaussian process classification; 5-HT$_{2A}$, serotonin 2A; LAM-KET, lamotrigine followed by ketamine infusion; MRI, magnetic resonance imaging; NMDA, *N*-methyl-D-aspartate; PCP, phencyclidine; phMRI, pharmacological MRI; PLA-SAL, placebo followed by saline infusion; PLA-KET, placebo followed by ketamine infusion; RIS-KET, risperidone followed by ketamine infusion; ROI, regions of interest; T$_{1/2}$, period of time over which the concentration of a drug decreases by half from a reference concentration.

2003; Gozzi et al., 2008; Hackler et al., 2010; Chin et al., 2011). In humans, one study to date has demonstrated modulation of the central response to ketamine challenge using neuroimaging (Deakin et al., 2008). Specifically, ketamine was infused intravenously during a resting-state pharmacological magnetic resonance imaging (phMRI) time series to directly measure the compound's effects on the regional blood oxygen level–dependent (BOLD) signal. The BOLD phMRI response to ketamine was attenuated by pretreatment with a single dose of lamotrigine (Deakin et al., 2008). Ketamine-induced increases in the clinician-administered dissociative states scales and brief psychosis rating scales were also reduced by lamotrigine, a finding consistent with a previous behavioral study (Anand et al., 2000). Given that lamotrigine inhibits the release of glutamate, it was concluded that the ketamine-induced change in both symptoms and BOLD signal (attenuated by lamotrigine) was due to an increase in glutamate release. This is consistent with rodent studies showing increased glutamate efflux in the prefrontal cortex upon acute administration of PCP (Moghaddam et al., 1997) and ketamine (Lorrain et al., 2003); interestingly, both of these studies also demonstrated reversal of this glutamate efflux by pretreatment with metabotropic glutamate 2/3 agonists, presumed to attenuate synaptic glutamate release. Additionally, in humans, the link between ketamine administration and cortical glutamate levels has recently been confirmed using magnetic resonance spectroscopy of the anterior cingulate gyrus (Stone et al., 2012).

In an open-label study, we recently replicated the BOLD phMRI response to ketamine in healthy humans using a subanesthetic dose demonstrating both group-level reproducibility and within-subject reliability (De Simoni et al., 2013). The aims of the present study were to 1) replicate the attenuation of the ketamine-induced BOLD phMRI signal changes using lamotrigine in a placebo-controlled, repeated-measures design in which all subjects receive treatments; 2) further validate the modulation of the ketamine-induced BOLD signal changes using an existing antipsychotic with a mechanism likely to modulate glutamate release; and 3) develop an analysis framework to benchmark the degree of attenuation of ketamine-induced BOLD signal changes. For the second aim, we selected the atypical antipsychotic risperidone, which has high affinities for dopamine $D_2$ and serotonin 2A (5-HT$_{2A}$) receptors. Risperidone achieves dopamine $D_2$ receptor occupancy in the range of clinical efficacy (>50%), while being well tolerated, after a single dose in healthy volunteers (Tauscher et al., 2004), and consistently achieves higher cortical occupancy of 5-HT$_{2A}$ receptors (Farde et al., 1995; Nyberg et al., 1999). 5-HT$_{2A}$ receptor antagonists are hypothesized to contribute to reductions in glutamate release in the cortex, in turn contributing to therapeutic efficacy in psychoses (Large, 2007). We thus expected risperidone to attenuate the effects of ketamine via this 5-HT$_{2A}$ antagonism (Meltzer et al., 2011).

Using conventional univariate statistics, we tested the modulatory effects in preselected regions of interest (ROIs) previously determined to show strong BOLD signal changes in response to ketamine administration (Deakin et al., 2008; De Simoni et al., 2013). Alternatively, pattern recognition approaches, which have not previously been evaluated in the context of resting-state phMRI, may be particularly useful because they 1) do not require ROI selection; 2) may be more sensitive than univariate approaches when the pharmacological

intervention elicits correlated, distributed effects across brain regions; and 3) reduce effects across brain regions to a single outcome measure based on the whole-brain pattern. This framework may have particular value for in vivo investigations in which participants are exposed to multiple sessions with different drug regimens, allowing the assessment of the mechanisms of action of drugs and their interactions with other compounds at a systems level.

Here, we build on our previous demonstration of a reliable ketamine phMRI response (De Simoni et al., 2013). Within a placebo-controlled design, we seek to replicate the reported attenuation of the ketamine effect by lamotrigine (Deakin et al., 2008), and investigate the effect of pretreatment with risperidone using both a univariate analysis and a bespoke multivariate framework. Based on previous studies (Anand et al., 2000; Large et al., 2005; Deakin et al., 2008; Gozzi et al., 2008; Meltzer et al., 2011), we expected that both lamotrigine and risperidone would attenuate the effects of ketamine on BOLD phMRI signal through glutamatergic modulation, albeit via different mechanisms of action.

## Materials and Methods

### Participants

Healthy male volunteers were recruited via advertisements and our volunteer database. Participants were screened for any history of psychiatric, neurologic, or physical illness. Other exclusion criteria included positive urine screen for drugs of abuse, out of range urinalysis or standard safety blood test results, consuming the equivalent of >5 caffeinated drinks per day, smoking >5 cigarettes per day, or taking prescribed or nonprescribed drugs. Following screening, 20 subjects entered the study. One volunteer withdrew after fainting upon cannulation (session 1), one withdrew due to nausea (session 3), and two others were withdrawn due to positive drug screening. Sixteen participants (mean age 25.8 years; S.D. = 5.7; range 20–37) completed all four sessions. All participants gave written informed consent. The study was approved by the Wandsworth Research Ethics Committee (09/H0803/48).

### Experimental Design

This randomized, placebo-controlled, partial crossover design involved screening and four scanning visits. Scanning visits were separated by at least 10 days, this being >5 times the longest plasma half-life ($T_{1/2}$) of the two orally administered compounds, where $T_{1/2}$ = 35 hours for lamotrigine (Cohen et al., 1987) and $T_{1/2}$ = 20 hours for risperidone (Huang et al., 1993). The $T_{max}$ (the time after administration of a drug when the maximum plasma concentration is reached) values for lamotrigine and risperidone were 1–2 hours and 1.4–4.8 hours, respectively.

At each visit, participants received a single oral dose of placebo or a study drug and a ketamine or saline infusion (both double blind). The four combinations administered were placebo (ascorbic acid) and saline infusion (PLA-SAL), placebo and ketamine infusion (PLA-KET), lamotrigine (300 mg) and ketamine infusion (LAM-KET), and risperidone (2 mg) and ketamine infusion (RIS-KET). Treatment order was randomized and balanced within a Latin-square design. The study day timeline is given in Fig. 1, with the imaging procedures performed during the broad maximum plasma exposure of both risperidone and lamotrigine (Cohen et al., 1987; Huang et al., 1993). Here, we report the results of the phMRI data only.

Blood samples were taken at 0.5, 1, 1.5, 4, and 8 hours following oral drug administration to determine the plasma pharmacokinetics of lamotrigine or risperidone, and at 15 and 75 minutes after commencing ketamine infusion to confirm target ketamine plasma levels. Heart rate and blood pressure measurements can be found in Supplemental Table 1. Subjective rating scales were also recorded.
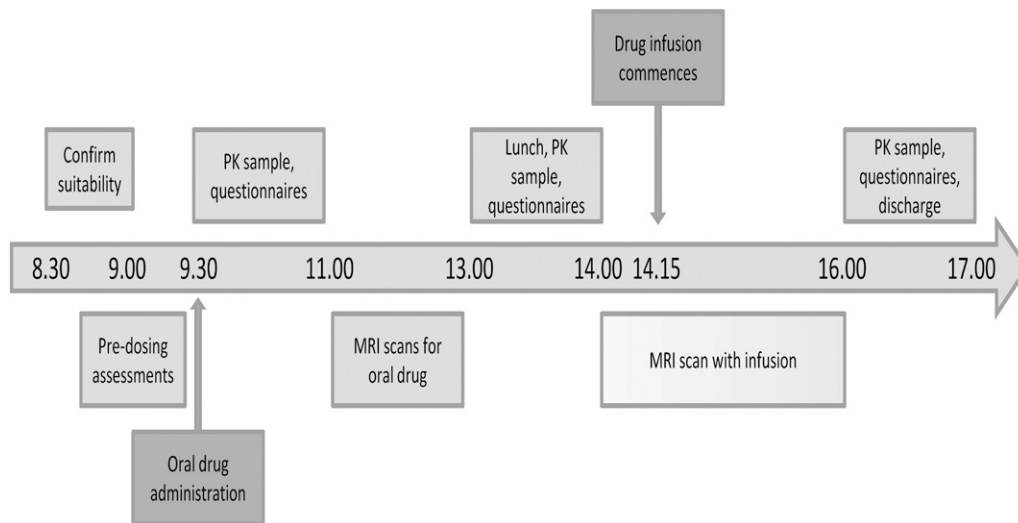
**Fig. 1.** Timeline of events on each study day. MRI scans acquired during the oral drug administration phase and infusion phase included cognitive functional MRI tasks and a breath-hold paradigm. Results from these analyses are not reported here. Times are shown in 24-hour clock convention. PK, pharmacokinetic.

**Ketamine Infusion.** Racemic ketamine (Ketalar; Pfizer, New York, NY) was administered intravenously based on the Clements 250 model (Absalom et al., 2007) and implemented in Stanpump (www.opentci.org) using a Graseby 3400 pump (Smiths Medical, Kent, UK) with a target plasma level of 75 ng/ml in accordance with the subject's height and weight (measured at each visit). The subanesthetic dose of ketamine delivered was (mean ± S.D.) 0.12 ± 0.003 mg/kg during the first minute followed by a pseudo-continuous infusion of approximately 0.31 mg/kg/h. This infusion paradigm was established in an independent cohort as inducing low levels of subjective effects, while eliciting a reliable phMRI response (De Simoni et al., 2013).

## Subjective Ratings

Subjective effects of ketamine were captured using a brief questionnaire, designed for rapid assessment, administered approximately 4 and 5 hours post oral dosing (just prior to ketamine infusion and approximately 20 minutes following initiation of ketamine infusion). The six items in this questionnaire were based on items from the Psychotomimetic States Inventory, clinician-administered dissociative states scales, and visual analog scales that demonstrated high and reliable sensitivity to the administration of ketamine in a separate cohort (De Simoni et al., 2013; see Supplemental Table 2).

## Image Acquisition

Participants were scanned using a 3.0T General Electric Signa HDx scanner (Milwaukee, WI). A 15-minute, eyes-open, resting-state BOLD phMRI scan was acquired using gradient-echo echo-planar imaging. A total of 450 image volumes of 38 near-axial slices (3-mm thickness, interslice gap of 0.3 mm aligned to the anterior commissure-posterior commissure) were acquired per session (time echo/repetition time = 30/2000 milliseconds, flip angle = 75°, in-plane resolution = 3.3 mm, matrix size = 64 × 64, field of view = 21.1 × 21.1cm). A higher-resolution gradient-echo scan was also acquired (43 3-mm-thick near-axial slices with 0.3-mm gap, time echo/repetition time = 30/2000 milliseconds, flip angle = 90°, in-plane resolution = 3.3 mm, matrix size = 128 × 128, field of view = 24 × 24 cm).

## Image Preprocessing and Modeling

PhMRI data were preprocessed using Statistical Parametric Mapping 5 (SPM5; www.fil.ion.ucl.ac.uk/spm). This involved slice-timing correction, realignment, coregistration to the high-resolution image, spatial normalization to the SPM echo-planar imaging template using parameters derived from nonlinear normalization of the high-resolution image, and spatial smoothing (8-mm full width at half maximum Gaussian kernel). A high-pass filter with a cutoff of 1200s (twice the postinfusion phMRI scan duration) was applied to the data to minimize the influence of very-low-frequency noise and scanner drift.

First-level modeling was performed in a general linear model framework, the design matrix which was determined in a previous study to reliably capture the ketamine phMRI response (De Simoni et al., 2013). This design matrix comprised the following regressors:

1. A gamma-variate (GV) function (Madsen, 1992) to model the phMRI response to ketamine

$$f(t) = \left(\frac{t}{t_{\max}}\right)^{t_{\max}\beta} e^{(t_{\max} - t)\beta}$$

where $t_{max}$ (set to 120, i.e., 240 seconds) relates to the time of the peak amplitude and $\beta$ (set to 0.01) is a "shape" parameter. This was preceded by a flat baseline modeling preinfusion (De Simoni et al., 2013).

1. The first component of a singular value decomposition of the 6 head motion traces; and
2. A linear drift term.

The beta images from the contrast of the first regressor were used in the group-level analyses.

## Group-Level Univariate Analysis

Atlas- and coordinate-based ROIs responsive to ketamine were prespecified based on previous studies (Deakin et al., 2008; De Simoni et al., 2013) (Supplemental Methods). These included the anterior cingulate cortex, supragenual paracingulate cortex, thalamus, posterior cingulate cortex, supplementary motor area, left anterior insula, right anterior insula, left operculum, right operculum, precuneus, and medial occipital lobes. Mean beta values were extracted from each ROI with SPM5 toolbox MarsBar from the first-level beta maps.

Statistical analysis of the ROI measures was performed in SAS version 9.1 (www.sas.com) using a mixed-effects model with treatment (fixed), session (fixed), ROI (fixed), and subject (random) as factors. Mean estimates for each treatment condition and the mean differences between treatment conditions, across ROIs, were generated for the following comparisons: PLA-KET versus LAM-KET, PLA-KET

versus RIS-KET, and PLA-SAL versus PLA-KET. Post-hoc comparisons by ROI were performed using analogous models.

Whole-brain univariate analyses were also performed using flexible factorial analysis of variance models in SPM with a statistical significance threshold of $P < 0.05$ (cluster corrected with a $P < 0.001$ voxelwise threshold).

## Group-Level Multivariate Analysis

We used Gaussian process classification (GPC), a probabilistic approach to classification that models the posterior probabilities of a class label $[1, -1]$ for an unseen test sample, given a set of training data (Rasmussen and Williams, 2006). For example, when training the GPC with a subset of the PLA-KET images (label: 1) and PLA-SAL images (label: $-1$), the GPC can then predict the probability of an unseen image belonging to the PLA-KET group while capturing the confidence of the predicted label. This is particularly useful for pharmacological modulation applications (Marquand et al., 2010), as it enables us to place an individual phMRI response on a continuum to gauge the extent of the modulation relative to a control condition (PLA-KET in this case). To assign a categorical label to an unseen test case, the predictive probability threshold was set at 0.5. A detailed account of GPC is provided in the Supplemental Data.

**Implementation of Gaussian Process Classification.** Given the repeated-measures nature of this study, the GPC was trained in a leave-one-out manner, whereby data from 15 of the participants were used to train the model, and the final (unseen) participant's data were used for testing. Additionally, the beta images were mean-centered (prior to classification) in a within-subject manner by subtracting from each voxel the mean across the contrast of interest images [e.g., for classification against the PLA-SAL–PLA-KET continuum, the mean per voxel of the PLA-SAL and PLA-KET conditions was subtracted from the images for all four conditions (Fig. 2)].

Statistical significance of the classification accuracies was assessed using permutation testing. The class labels were randomly permuted 1000 times, and the classifier was retrained using these labels to create a probability distribution of the accuracy.

Two group-level contrasts were investigated using the classifier:

1. The classifier was trained on PLA-SAL and PLA-KET images and then tested on all four conditions for the remaining unseen subject. This allowed the RIS-KET and LAM-KET scans to be positioned on the PLA-SAL–PLA-KET continuum.
2. The classifier was trained on the LAM-KET (or RIS-KET) and PLA-KET images and tested only on the corresponding LAM-KET (or RIS-KET) and PLA-KET from the unseen subject. This directly tested the modulation of the ketamine response by lamotrigine (or risperidone) in the absence of the PLA-SAL infusion scans.

Multivariate maps (g-maps) were constructed to visualize the spatial pattern driving the classification. For the g-map, training samples contribute in proportion to how representative they are of their respective class (Marquand et al., 2010). Since multivariate techniques are sensitive to spatial correlation, and the performance of the classifier is based on the entire pattern rather than individual voxels, inference based on local regions should be avoided when interpreting these maps (see Supplemental Methods).

## Results

**Pharmacokinetics.** The mean and standard deviations of plasma concentration of ketamine pretreatment were (in ng/ml) $62.7 \pm 17.6$ (PLA-KET), $66.1 \pm 22.1$ (LAM-KET), and
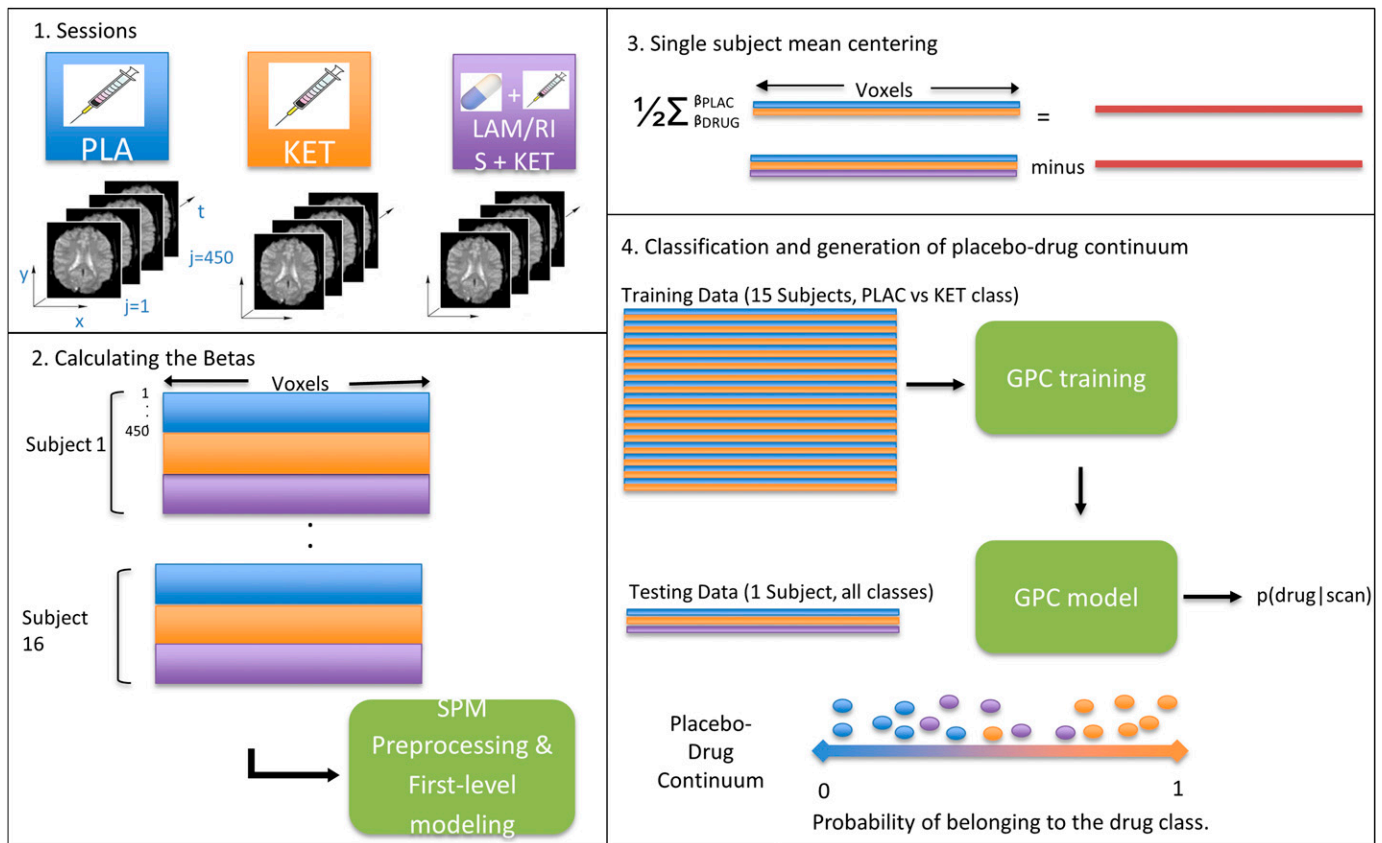


**Fig. 2.** Analysis pipeline. (1) Experimental setup. (2) Univariate analysis; incorporating image preprocessing and general linear model analysis. (3) Data preparation prior to pattern recognition which exploits the repeated-measures design. (4) Training and testing of the GPC models created per subject and an illustration of the PLA-KET continuum. PLAC, placebo.

49.1 ± 15.9 (RIS-KET) after 15 minutes of infusion (concentration of KET was significantly different for RIS-KET compared with PLA-KET; $P = 0.02$ by Wilcoxon rank sum), and 72.8 ± 20.8 (PLA-KET), 71.9 ± 35.5 (LAM-KET), and 77.8 ± 26.9 (RIS-KET) after 75 minutes of infusion. Maximum risperidone concentrations were achieved between 1 and 4.5 hours post dose (median of 2 hours). Geometric mean (geometric percent coefficient of variation) area under the curve (AUC)[0–4.5 hours] and AUC[0–8 hours] estimates of risperidone concentration were 40.0 (79) and 61.7 (83) ng · h/ml, respectively. Similarly, maximum lamotrigine concentrations were achieved between 1 and 4.5 hours post dose (median of 1.75 hours). Geometric mean AUC[0–4.5 hours] and AUC[0–8 hours] estimates of lamotrigine concentration were 14,125 (16) and 26,018 (17) ng · h/ml, respectively. The pharmacokinetic profiles of both compounds described a broad plateau following $T_{max}$, consistent with previously described elimination times.

**Univariate Analysis.** The ROI analysis revealed a significant BOLD response to ketamine infusion relative to saline ($P < 0.001$; Tables 1–3). This included both positive (Tables 1 and 2) and negative (Table 3) BOLD changes. For the positively responding regions, pretreatment with both lamotrigine and risperidone resulted in a relatively consistent attenuation of the ketamine responses intermediate between the PLA-SAL and PLA-KET conditions ($P < 0.001$ for both lamotrigine and risperidone) (Fig. 3, A and C). BOLD time series from two ROIs which are representative of all positively responding regions are shown in Fig. 4. For the negatively responding regions in the subgenual cingulate and ventromedial prefrontal cortex, risperidone strongly attenuated the negative BOLD response ($P < 0.001$), whereas the effect of lamotrigine was weaker ($P = 0.046$). Only this region differed between the pretreatment conditions ($P = 0.042$). In the striatum, neither risperidone nor lamotrigine attenuated the response to ketamine (post-hoc $t$ tests; $P > 0.15$). Whole-brain maps of PLA-SAL contrasted with PLA-KET, and PLA-KET contrasted with both LAM-KET and RIS-KET is provided in Supplemental Fig. 1.

**Multivariate Whole-Brain Analysis.** The GPC was applied to the whole-brain beta images to provide categorical classification labels, i.e., PLA-SAL or PLA-KET, and predictive probabilities of KET infusion. The classifier was initially trained on the PLA-SAL versus PLA-KET condition and then tested on all four conditions for the unseen subject (see Table 4). Perfect classification (100%) was achieved for PLA-SAL versus PLA-KET. Lamotrigine pretreatment resulted in a reduced accuracy of 87.5%, with 4 out of 16 of the subjects in the LAM-KET class being labeled as PLA-SAL.

Risperidone pretreatment also resulted in reduced accuracy (75%), with 8 out of 16 of the subjects in the RIS-KET class being labeled as PLA-SAL.

The mean posterior probabilities of belonging to the PLA-KET group (Fig. 5A) showed a marked reduction with both LAM (mean 0.58) and RIS (mean 0.49) pretreatment. The comparisons between PLA-KET versus LAM-KET and PLA-KET versus RIS-KET were both highly significant (Wilcoxon rank sum test, $P = 0.00042$ and $P = 0.00036$, respectively). There was no statistically significant difference between the LAM-KET versus RIS-KET conditions.

In Fig. 5B, the PLA-SAL to PLA-KET continuum illustrates an excellent separation between the PLA-SAL and PLA-KET groups, with only one subject close to misclassification. The LAM-KET predictive probabilities are widely spread across the continuum (0.10–0.97, mean = 0.58), similar to the RIS-KET predictive probabilities (0.01–0.90, mean = 0.49). The distributed patterns of brain regions (the g-map) driving the discrimination between PLA-SAL and PLA-KET are illustrated in Fig. 6. The g-map shows a striking similarity to the univariate map of the same contrast (Supplemental Fig. 1).

To directly investigate the attenuation of the ketamine response, we classified LAM-KET and RIS-KET against PLA-KET. Here, high classification accuracy indicates that the pretreated scans are dissimilar to the PLA-KET condition. The performance of the classifiers for LAM-KET and RIS-KET conditions versus PLA-KET were significantly above chance ($P < 0.05$), 68.8 and 81.3%, respectively (see Supplemental Table 3). The g-maps for both models can be seen in Supplemental Figs. 2 and 3. Both maps appear to be highly similar, indicating that the distributed ketamine response was broadly attenuated by both LAM and RIS pretreatment.

**Subjective Ratings.** Participants reported feeling less alert and clear-headed after ketamine infusion (pre- versus post-infusion). Pretreatment with lamotrigine and risperidone resulted in no significant effect of ketamine on the alert-drowsy scale, whereas significant differences remained for the muzzy-clear scale (see Supplemental Results, which includes Supplemental Figs. 4 and 5 and Table 4).

**Correlations between Pharmacokinetic and phMRI Responses.** No significant correlations were found between ketamine plasma levels and either the BOLD phMRI changes or predictive probabilities from the GPC (see Supplemental Data).

To explore whether the response to risperidone pretreatment was related to the response to lamotrigine pretreatment and investigate potential shared mechanistic endpoints, we also tested the correlation between the predictive probabilities of belonging to the ketamine class for the two pretreatments.

TABLE 1

Comparison of LS mean difference across all anatomic ROIs (excluding caudate and putamen)

ROIs included the anterior cingulate cortex, supragenual paracingulate gyrus, thalamus, posterior cingulate cortex, supplementary motor area, insula left, insula right, operculum left, operculum right, precuneus, and medial occipital lobes.

| N | Treatment | LS Mean (95% CI) | Contrast | | |
|---|---|---|---|---|---|
| | | | Paired Comparison | Difference (95% CI) | $P$ |
| 16 | PLA-KET | 2.4211 (2.0404, 2.8018) | PK–PS | 2.5283 (2.2927, 2.7639) | <0.001 |
| 16 | LAM-KET | 1.3788 (0.9981, 1.7595) | PK–LK | 1.0423 (1.2780, 0.8067) | <0.001 |
| 16 | RIS-KET | 1.0416 (0.6609, 1.4222) | PK–RK | 1.3796 (1.6152, 1.1439) | <0.001 |
| 16 | PLA-SAL | −0.1072 (−0.4879, 0.2735) | | | |

CI, confidence interval; LK, lamotrigine + ketamine; LS, least square; N, number of subjects; PK, placebo + ketamine; PS, placebo + saline; RK, risperidone + ketamine; ROI, region of interest.

TABLE 2

Comparison of LS mean difference across all positive-responding coordinate ROIs

ROIs included the anterior cingulate cortex, medial prefrontal cortex, right dorsolateral prefrontal cortex, right ventrolateral prefrontal cortex, left parahippocampal gyrus, right parahippocampal gyrus, and mid-cingulate cortex.

| N | Treatment | LS Mean (95% CI) | Contrast | | |
|---|---|---|---|---|---|
| | | | Paired Comparison | Difference (95% CI) | p |
| 16 | PLA-KET | 3.2793 (2.7313, 3.8273) | PK–PS | 3.4505 (2.9890, 3.9120) | <0.001 |
| 16 | LAM-KET | 1.9209 (1.3728, 2.4689) | PK–LK | 1.3584 (1.8199, 0.8969) | <0.001 |
| 16 | RIS-KET | 1.5085 (0.9605, 2.0565) | PK–RK | 1.7708 (2.2323, 1.3093) | <0.001 |
| 16 | PLA-SAL | −0.1712 (-0.7192, 0.3768) | | | |

CI, confidence interval; LK, lamotrigine + ketamine; LS, least square; N, number of subjects; PK, placebo + ketamine; PS, placebo + saline; RK, risperidone + ketamine; ROI, region of interest.

A significant correlation was found (Spearman's rho = 0.61, $P = 0.014$).

## Discussion

We found that lamotrigine and the antipsychotic risperidone attenuated the phMRI response to ketamine to a similar degree. This was demonstrated using both univariate analyses of predefined ROIs (Deakin et al., 2008; De Simoni et al., 2013) and a novel application of multivariate pattern analysis to the whole-brain phMRI response. The latter approach may have particular value for in vivo investigation of mechanisms of action of existing and novel compounds at a systems level.

In the univariate analysis, lamotrigine and risperidone attenuated the ketamine effect across most ROIs, including the medial prefrontal and cingulate regions and the thalamus. Using multivariate analysis, the predictive probability of belonging to the ketamine class (without pretreatment) was computed across all four conditions. The phMRI response to ketamine is known to be strong (Deakin et al., 2008; De Simoni et al., 2013), and this was reflected in the correct discrimination of all placebo-saline from placebo-ketamine conditions, thus providing a robust assay to investigate modulation by pharmacological pretreatment.

Pretreatment with either lamotrigine or risperidone resulted in attenuation of the phMRI response to ketamine (benchmarked against the predictive probability of belonging to the ketamine class). Indeed, both lamotrigine and risperidone pretreatment resulted in phMRI responses to ketamine that were more difficult to separate from the saline condition than ketamine alone. Although the accuracies, predictive probabilities, and univariate maps (Supplemental Fig. 1) suggested that risperidone was slightly more effective in attenuating the positive ketamine phMRI response, there was no difference when these two conditions were contrasted directly using the GPC (56% accuracy; see Supplemental Data), and the predictive probabilities between these two conditions were correlated. ROI analysis showed that only risperidone pretreatment blocked the subgenual prefrontal cortex response to ketamine, a region that may be important in understanding antidepressant effects of treatments (Agid et al., 2007). Direct comparison between the LAM-KET and RIS-KET responses in these ROIs using post-hoc $t$ tests revealed a significant difference in the subgenual cingulate, with risperidone having the larger effect. Interestingly, the subgenual prefrontal cortex has a particularly high innervation of serotonin (5-HT) neurons indicated by binding of [3H]Citalopram, suggesting serotonergic mechanisms may play a role in the effects of acute ketamine within this region (Mantere et al., 2002; Varnas et al., 2004) and the attenuation of these effects with risperidone. This, however, remains speculative, with formal testing using selective 5-HT$_{2A}$ antagonists required. Overall, this indicates that risperidone and lamotrigine produce a global attenuation of the positive ketamine response in contrast to the selective attenuation with risperidone of the subgenual response.

Lamotrigine is a broad-spectrum anticonvulsant that inhibits voltage-gated ion channels, including sodium and calcium, with downstream effects resulting in inhibition of glutamate release (Large et al., 2005). Our findings are in keeping with previous studies in experimental animals and humans. In animals, acute administration of lamotrigine produced widespread inhibition of the relative cerebral blood volume response to the NMDA receptor antagonist PCP in all activated regions (Gozzi et al., 2008). When administered prior to a ketamine challenge in healthy volunteers, lamotrigine has been shown to reverse ketamine's effects on behavioral and cognitive measures (Anand et al., 2000) and reduce the ketamine-induced changes in the BOLD signal (Deakin et al., 2008).

This is the first study to investigate pretreatment with risperidone on the BOLD signal response to ketamine in healthy volunteers. In addition to its serotonergic effects,

TABLE 3

Comparison of LS mean difference across the two negative-responding coordinate ROIs

ROIs include the subgenual cingulate cortex coordinates from De Simoni et al. (2013) and Deakin et al. (2008).

| N | Treatment | LS Mean (95% CI) | Contrast | | |
|---|---|---|---|---|---|
| | | | Paired Comparison | Difference (95% CI) | P |
| 16 | PLA-KET | −5.0929 (-6.7774, -3.4084) | PK–PS | −4.9542 (-6.6589, -3.2495) | <0.001 |
| 16 | LAM-KET | −3.3569 (-5.0414, -1.6725) | PK–LK | −1.7360 (-0.0313, -3.4407) | 0.046 |
| 16 | RIS-KET | −0.2679 (-1.9523, 1.4166) | PK–RK | −4.8251 (-3.1204, -6.5297) | <0.001 |
| 16 | PLA-SAL | −0.1387 (-1.8232, 1.5458) | | | |

CI, confidence interval; LK, lamotrigine + ketamine; LS, least square; N, number of subjects; PK, placebo + ketamine; PS, placebo + saline; RK, risperidone + ketamine; ROI, region of interest.
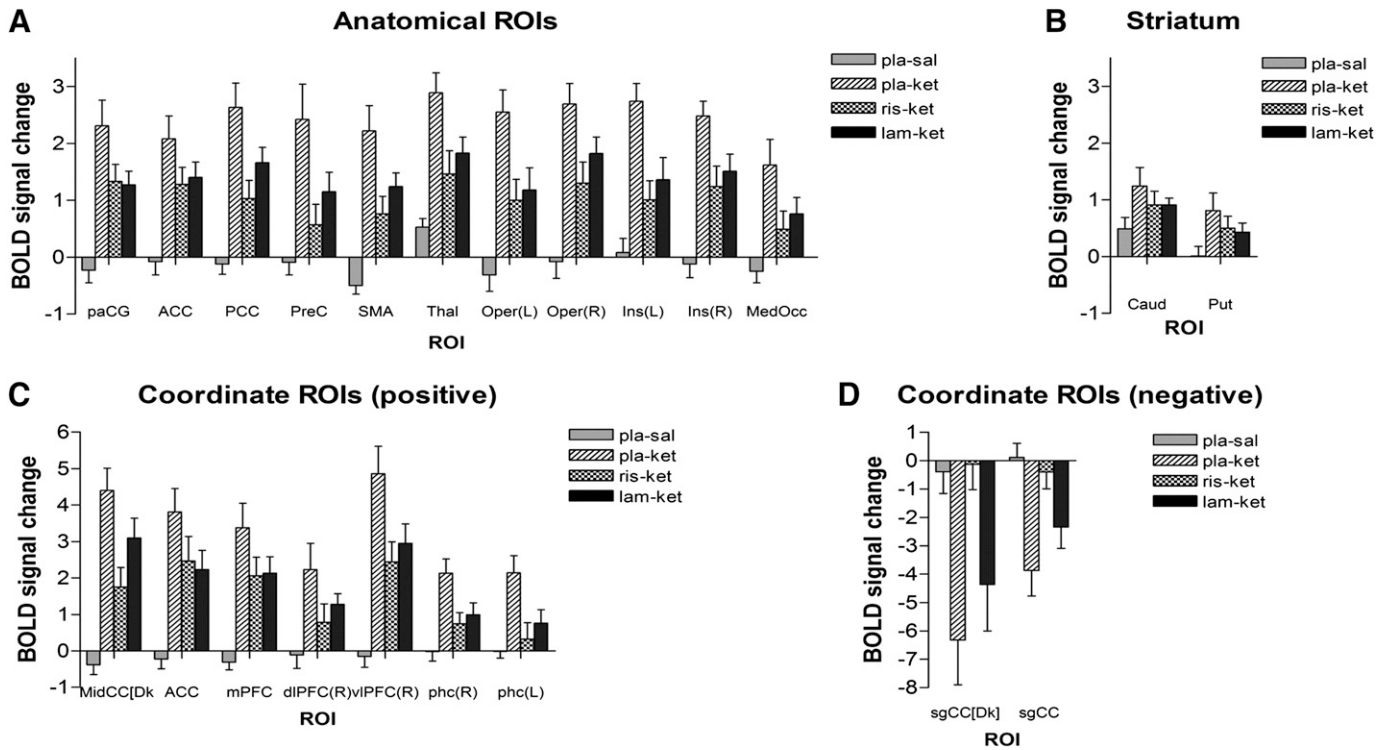
**Fig. 3.** Univariate responses by treatment condition for preselected ROIs (mean ± S.E.M. across subjects). The annotation "[Dk]" identifies coordinates specified based on Deakin et al. (2008). (A) Anatomic ROIs corresponding to brain regions strongly responding to the ketamine challenge. (B) Anatomic ROIs from the dorsal striatum to interrogate any preferential effect of risperidone due to its D2 antagonist properties. (C) Coordinate-based ROIs corresponding to foci of strong response to the ketamine challenge in a preparatory pilot study. (D) Coordinate-based ROIs corresponding to foci of strong negative BOLD responses to the ketamine challenge observed in a separate cohort (De Simoni et al., 2013) and in Deakin et al. (2008). ACC, anterior cingulate cortex; Caud, caudate; dlPFC(R), dorsolateral prefrontal cortex (right); Ins(L), anterior insula (left); Ins(R), anterior insula (right); MedOcc, medial occipital lobes; MidCC, mid-cingulate cortex; mPFC, medial prefrontal cortex; Oper(L), operculum (left); Oper(R), operculum (right); paCG, supragranular paracingulate gyrus; PCC, posterior cingulate cortex; phc(L), parahippocamPLA gyrus (left); phc(R), parahippocamPLA gyrus (right); PreC, precuneus; Put = putamen; sgCC, subgenual cingulate cortex; SMA, supplementary motor area; Thal, thalamus; vlPFC(R), ventrolateral prefrontal cortex (right). See *Materials and Methods* for a description of ROI definitions.

risperidone has high affinity for dopamine D2 receptors, which may conceivably have an impact on its interaction with ketamine. However, studies using selective D2 antagonists, such as haloperidol or raclopride, have failed to demonstrate a modulation of the effects of ketamine or PCP (Krystal et al., 1999; Gozzi et al., 2008; Oranje et al., 2009). Furthermore, no effects were observed in the striatum on the ketamine-induced BOLD changes following risperidone. Given the high density of dopamine D2 receptors in the striatum, this supports the proposal that antagonism at 5-HT$_{2A}$ receptors

is the prevailing mechanism underlying the risperidone-induced attenuation of the ketamine BOLD response via attenuated glutamate release (Adams and Moghaddam, 1998; Aghajanian and Marek, 2000; Large, 2007). Indeed, 5-HT$_{2A}$ selective antagonists and risperidone itself can block NMDA receptor antagonist–induced deficits in locomotor function (Meltzer et al., 2011) and cognitive function (Varty et al., 1999; Mirjana et al., 2004; Didriksen et al., 2007), deficits thought to be the result of a frontal hyperglutamatergic state.
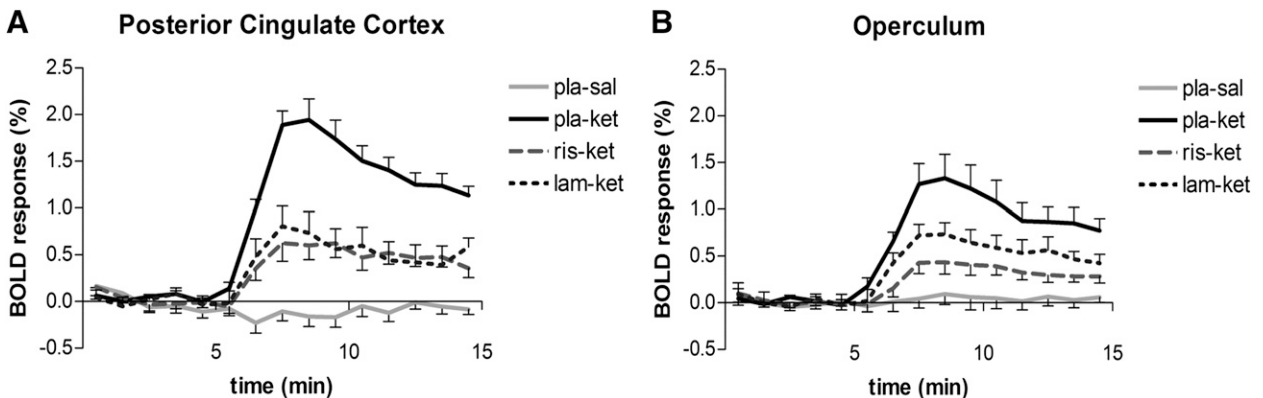


**Fig. 4.** BOLD signal time courses from the posterior cingulate cortex (A) and bilateral operculum (B). Mean ± S.E.M. across subjects for each treatment condition.

TABLE 4
Classification performance for the models trained on a static contrast and tested on three of the contrasts

The nomenclature p(y = *PLA-KET*|$x_{*-KET}$) implies the probability of belonging to the PLA-KET class given conditions where ketamine has been administered but the pretreatment (PLA, RIS, LAM) varies. Similarly, p(y = *PLA-KET*|$x_{PLA-SAL}$) denotes the probability of belonging to the ketamine class given the PLA-SAL condition, and is reported as the mean ± S.D.

| | Training Contrast | Test Contrast | | |
|---|---|---|---|---|
| | | PLA-SAL versus PLA-KET | PLA-SAL versus LAM-KET | PLA-SAL versus RIS-KET |
| Accuracy (%) | PLA-SAL versus PLA-KET | 100 | 87.5 | 75.0 |
| Sensitivity (%) | PLA-SAL versus PLA-KET | 100 | 75.0 | 50 |
| Specificity (%) | PLA-SAL versus PLA-KET | 100 | 100 | 100 |
| p(y = *PLA-KET*\|$x_{*-KET}$) | PLA-SAL versus PLA-KET | 0.88 ± 0.14 | 0.58 ± 0.56 | 0.49 ± 0.34 |
| p(y = *PLA-KET*\|$x_{PLA-SAL}$) | PLA-SAL versus PLA-KET | 0.12 ± 0.14 | 0.12 ± 0.14 | 0.12 ± 0.14 |

We cannot rule out that the main effects of lamotrigine and risperidone might influence the measurement of the ketamine response, even though it was derived relative to the preinfusion baseline. Given that the BOLD signal is nonquantitative, the preinfusion baseline cannot be compared directly across conditions, thus further experiments would be required to delineate the main effects of both pretreatments using, for example, dual-echo acquisition, which simultaneously acquires BOLD and quantitative perfusion signals (Wong et al., 1997).

Direct pharmacological effects on the vasculature represent a possible confound in the interpretation of our results. However, there are a number of reasons why vascular effects cannot explain our findings. First, the effects of ketamine alone match earlier observations using metabolism markers (2-deoxyglucose autoradiography in the rodent and fluorodeoxyglucose positron emission tomography in humans) (Duncan et al., 1998b; Langsjo et al., 2004). Second, we observed both increases and decreases in the BOLD signal response to ketamine, which is difficult to understand in a purely vascular framework. Third, a vascular account would predict differential effects based on the distribution of pharmacological targets. For example, risperidone would be predicted

to have a greater effect in areas of high dopamine receptor density, such as the striatum [dopamine is known to modulate vasodilation and constriction directly (Krimer et al., 1998)]. Instead, the observed attenuation of the ketamine-induced response to lamotrigine and risperidone was highly similar.

Another potential limitation is that the plasma levels of ketamine during the risperidone arm were significantly lower than the other study arms in the 15-minute sample. This may be because of the enzyme CYP3A4, which is known to metabolize both risperidone and ketamine (Fang et al., 1999). Thus, it is possible that the attenuation of the ketamine effect is via an increased enzymatic activity induced by risperidone, resulting in a lower delivered dose of ketamine. However, the ketamine levels were assessed after the phMRI scan from which the results were derived. It is not known whether the lower levels would have been present during the administration. Also, an explanation based purely on ketamine exposure is not supported by the data, as the degree of attenuation is not correlated with the plasma levels of ketamine.

Outside of its antagonist activity at NMDA receptors, ketamine also has effects at $\mu$-opioid receptors, acts as an inhibitor at serotonin and noradrenaline reuptake sites, interacts
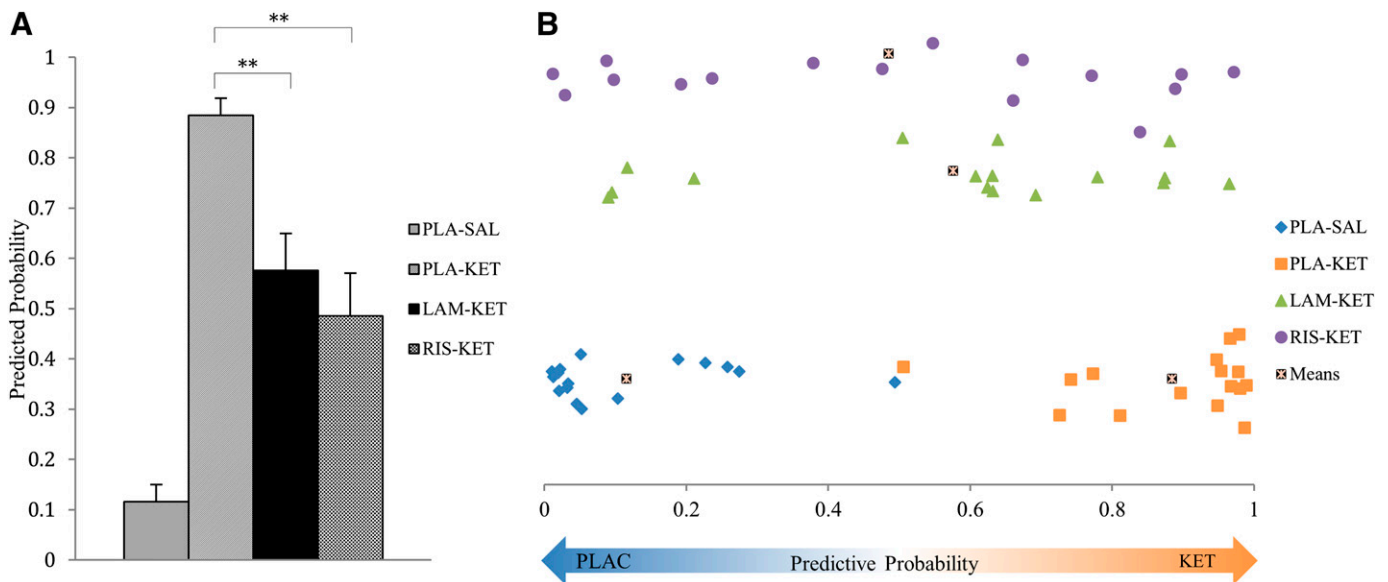
**Fig. 5.** (A) Posterior probability of belonging to the PLA-KET treatment class for each drug contrast. Probability of belonging to the ketamine class: ***$P <$ 0.001 (B) Placebo-to-ketamine continuum derived from the output of the GPC. A p(Ket|x*) (probability of belonging to the ketamine class given the test data x*) close to 1 implies a high probability of belonging to the ketamine class, and a p(Ket|x*) close to zero implies a high probability of belonging to the placebo class. The *y*-axis is used to separate the groups into three rows, with some jitter added to each row for visualization.
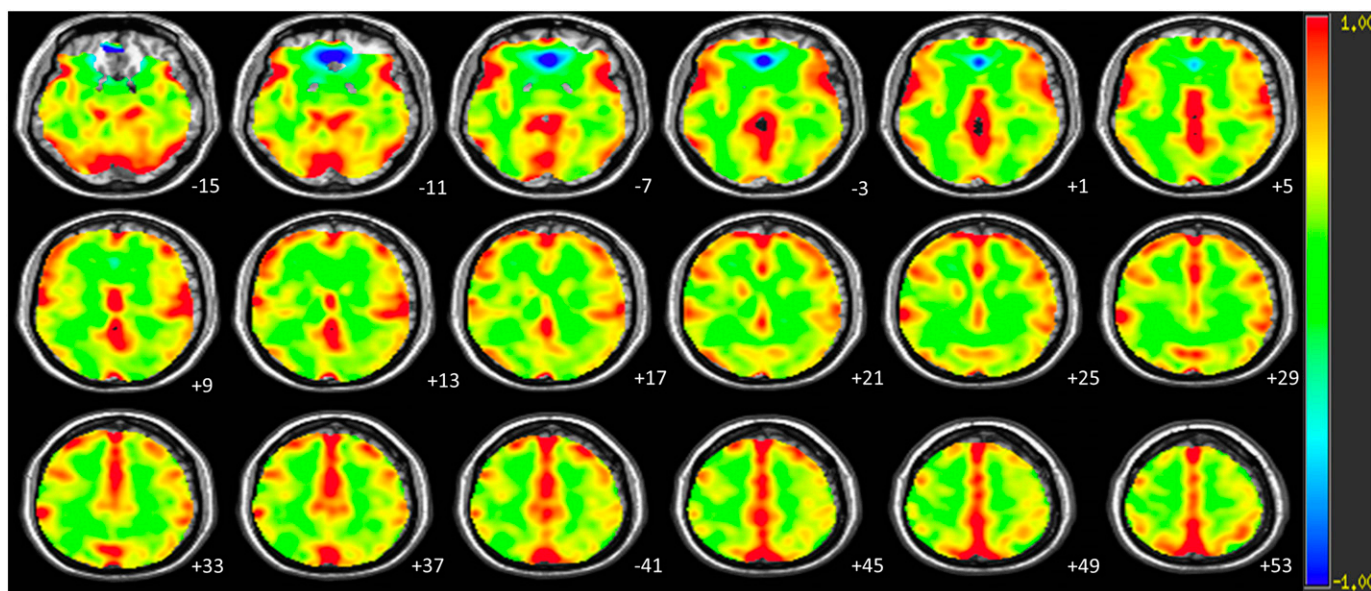
**Fig. 6.** Multivariate map (g-map) from the GPC which contrasts PLA-KET (class label: +1) and PLA-SAL (class label: −1). A positive g-map coefficient for a particular voxel indicates a higher overall beta score for the PLA-KET class (+1), and similarly, a negative g-map coefficient indicates a higher overall beta score for the PLA-SAL class (−1). The right-hand side of each image corresponds to the participants' right side with the transaxial slice numbers in Montreal Neurological Institute (MNI) coordinates (z-axis) shown in white.

with cholinergic and sigma receptors, and affects the dopamine system (Freeman and Bunney, 1984; Schmidt and Fadayel, 1996; Kapur and Seeman, 2002). Such effects have been described at higher doses and in relation to analgesia, although it remains possible that non-NMDA effects contributed to the changes observed in this study. More selective compounds aimed at modulating glutamate and other systems are required to fully characterize the ketamine-induced changes in BOLD signal.

## Conclusions

We have confirmed robust BOLD signal changes following acute administration of the NMDA antagonist ketamine, which can create a cluster of symptoms redolent of schizophrenia. Our analysis framework provided a clear demonstration of both a ketamine effect when contrasted against placebo, and an attenuation of this response with both lamotrigine and risperidone pretreatment. Our data also suggest serotonergic mechanisms play a role in the ketamine-induced subgenual cingulate changes, with potential relevance for understanding its antidepressant effects. This extends our previous work showing good reliability of the ketamine phMRI assay (De Simoni et al., 2013), and provides an analytical methodology to investigate the mechanistic action of novel compounds and inform important questions such as dose selection, particularly for compounds that do not rely on dopamine $D_2$ receptor blockade.

### Acknowledgments

### Authorship Contributions

*Participated in research design:* De Simoni, Brittain, Schwarz, Mehta, Williams, O'Daly.

*Conducted experiments:* De Simoni, Mehta.

*Contributed new reagents or analytic tools:* Doyle.

*Performed data analysis:* Doyle, De Simoni, Brittain.

*Wrote or contributed to the writing of the manuscript:* Doyle, De Simoni, Schwarz, Brittain, O'Daly, Williams, Mehta.

### References

Absalom AR, Lee M, Menon DK, Sharar SR, De Smet T, Halliday J, Ogden M, Corlett P, Honey GD, and Fletcher PC (2007) Predictive performance of the Domino, Hijazi, and Clements models during low-dose target-controlled ketamine infusions in healthy volunteers. *Br J Anaesth* **98**:615–623.

Adams B and Moghaddam B (1998) Corticolimbic dopamine neurotransmission is temporally dissociated from the cognitive and locomotor effects of phencyclidine. *J Neurosci* **18**:5545–5554.

Aghajanian GK and Marek GJ (2000) Serotonin model of schizophrenia: emerging role of glutamate mechanisms. *Brain Res Brain Res Rev* **31**:302–312.

Agid Y, Buzsáki G, Diamond DM, Frackowiak R, Giedd J, Girault JA, Grace A, Lambert JJ, Manji H, and Mayberg H, et al. (2007) How can drug discovery for psychiatric disorders be improved? *Nat Rev Drug Discov* **6**:189–201.

Anand A, Charney DS, Oren DA, Berman RM, Hu XS, Cappiello A, and Krystal JH (2000) Attenuation of the neuropsychiatric effects of ketamine with lamotrigine: support for hyperglutamatergic effects of N-methyl-D-aspartate receptor antagonists. *Arch Gen Psychiatry* **57**:270–276.

Chin CL, Upadhyay J, Marek GJ, Baker SJ, Zhang M, Mezler M, Fox GB, and Day M (2011) Awake rat pharmacological magnetic resonance imaging as a translational pharmacodynamic biomarker: metabotropic glutamate 2/3 agonist modulation of ketamine-induced blood oxygenation level dependence signals. *J Pharmacol Exp Ther* **336**:709–715.

Cohen AF, Land GS, Breimer DD, Yuen WC, Winton C, and Peck AW (1987) Lamotrigine, a new anticonvulsant: pharmacokinetics in normal humans. *Clin Pharmacol Ther* **42**:535–541.

De Simoni S, Schwarz AJ, O'Daly OG, Marquand AF, Brittain C, Gonzales C, Stephenson S, Williams SC, and Mehta MA (2013) Test-retest reliability of the BOLD pharmacological MRI response to ketamine in healthy volunteers. *Neuroimage* **64**:75–90.

Deakin JF, Lees J, McKie S, Hallak JE, Williams SR, and Dursun SM (2008) Glutamate and the neural basis of the subjective effects of ketamine: a pharmaco-magnetic resonance imaging study. *Arch Gen Psychiatry* **65**:154–164.

Didriksen M, Skarsfeldt T, and Arnt J (2007) Reversal of PCP-induced learning and memory deficits in the Morris' water maze by sertindole and other antipsychotics. *Psychopharmacology (Berl)* **193**:225–233.

Duncan GE, Leipzig JN, Mailman RB, and Lieberman JA (1998a) Differential effects of clozapine and haloperidol on ketamine-induced brain metabolic activation. *Brain Res* **812**:65–75.

Duncan GE, Miyamoto S, Leipzig JN, and Lieberman JA (2000) Comparison of the effects of clozapine, risperidone, and olanzapine on ketamine-induced alterations in regional brain metabolism. *J Pharmacol Exp Ther* **293**:8–14.

Duncan GE, Moy SS, Knapp DJ, Mueller RA, and Breese GR (1998b) Metabolic mapping of the rat brain after subanesthetic doses of ketamine: potential relevance to schizophrenia. *Brain Res* **787**:181–190.

Fang J, Bourin M, and Baker GB (1999) Metabolism of risperidone to 9-hydroxyrisperidone by human cytochromes P450 2D6 and 3A4. *Naunyn Schmiedebergs Arch Pharmacol* **359**:147–151.

Farber NB, Wozniak DF, Price MT, Labruyere J, Huss J, St Peter H, and Olney JW (1995) Age-specific neurotoxicity in the rat associated with NMDA receptor blockade: potential relevance to schizophrenia? *Biol Psychiatry* **38**:788–796.

Farde L, Nyberg S, Oxenstierna G, Nakashima Y, Halldin C, and Ericsson B (1995) Positron emission tomography studies on D2 and 5-HT2 receptor binding in risperidone-treated schizophrenic patients. *J Clin Psychopharmacol* **15**(1, Suppl 1) 19S–23S.

Freeman AS and Bunney BS (1984) The effects of phencyclidine and N-allylnormetazocine on midbrain dopamine neuronal activity. *Eur J Pharmacol* **104**:287–293.

Gozzi A, Large CH, Schwarz A, Bertani S, Crestan V, and Bifone A (2008) Differential effects of antipsychotic and glutamatergic agents on the phMRI response to phencyclidine. *Neuropsychopharmacology* **33**:1690–1703.

Hackler EA, Byun NE, Jones CK, Williams JM, Baheza R, Sengupta S, Grier MD, Avison M, Conn PJ, and Gore JC (2010) Selective potentiation of the metabotropic glutamate receptor subtype 2 blocks phencyclidine-induced hyperlocomotion and brain activation. *Neuroscience* **168**:209–218.

Huang ML, Van Peer A, Woestenborghs R, De Coster R, Heykants J, Jansen AA, Zylicz Z, Visscher HW, and Jonkman JH (1993) Pharmacokinetics of the novel antipsychotic agent risperidone and the prolactin response in healthy subjects. *Clin Pharmacol Ther* **54**:257–268.

Kapur S and Seeman P (2002) NMDA receptor antagonists ketamine and PCP have direct effects on the dopamine D(2) and serotonin 5-HT(2)receptors-implications for models of schizophrenia. *Mol Psychiatry* **7**:837–844.

Krimer LS, Muly EC, 3rd, Williams GV, and Goldman-Rakic PS (1998) Dopaminergic regulation of cerebral cortical microcirculation. *Nat Neurosci* **1**:286–289.

Krystal JH, D'Souza DC, Karper LP, Bennett A, Abi-Dargham A, Abi-Saab D, Cassello K, Bowers MB, Jr, Vegso S, and Heninger GR, et al. (1999) Interactive effects of subanesthetic ketamine and haloperidol in healthy humans. *Psychopharmacology (Berl)* **145**:193–204.

Krystal JH, Karper LP, Seibyl JP, Freeman GK, Delaney R, Bremner JD, Heninger GR, Bowers MB, Jr, and Charney DS (1994) Subanesthetic effects of the non-competitive NMDA antagonist, ketamine, in humans. Psychotomimetic, perceptual, cognitive, and neuroendocrine responses. *Arch Gen Psychiatry* **51**:199–214.

Långsjö JW, Salmi E, Kaisti KK, Aalto S, Hinkka S, Aantaa R, Oikonen V, Viljanen T, Kurki T, and Silvanto M, et al. (2004) Effects of subanesthetic ketamine on regional cerebral glucose metabolism in humans. *Anesthesiology* **100**:1065–1071.

Large CH (2007) Do NMDA receptor antagonist models of schizophrenia predict the clinical efficacy of antipsychotic drugs? *J Psychopharmacol* **21**:283–301.

Large CH, Webster EL, and Goff DC (2005) The potential role of lamotrigine in schizophrenia. *Psychopharmacology (Berl)* **181**:415–436.

Lorrain DS, Baccei CS, Bristow LJ, Anderson JJ, and Varney MA (2003) Effects of ketamine and N-methyl-D-aspartate on glutamate and dopamine release in the rat prefrontal cortex: modulation by a group II selective metabotropic glutamate receptor agonist LY379268. *Neuroscience* **117**:697–706.

Madsen MT (1992) A simplified formulation of the gamma variate function. *Phys Med Biol* **37**:1597–1600 DOI: 10.1088/0031-9155/37/7/010.

Mantere T, Tupala E, Hall H, Särkioja T, Räsänen P, Bergström K, Callaway J, and Tiihonen J (2002) Serotonin transporter distribution and density in the cerebral cortex of alcoholic and nonalcoholic comparison subjects: a whole-hemisphere autoradiography study. *Am J Psychiatry* **159**:599–606.

Marquand A, Howard M, Brammer M, Chu C, Coen S, and Mourão-Miranda J (2010) Quantitative prediction of subjective pain intensity from whole-brain fMRI data using Gaussian processes. *Neuroimage* **49**:2178–2189.

Meltzer HY, Horiguchi M, and Massey BW (2011) The role of serotonin in the NMDA receptor antagonist models of psychosis and cognitive impairment. *Psychopharmacology (Berl)* **213**:289–305.

Mirjana C, Baviera M, Invernizzi RW, and Balducci C (2004) The serotonin 5-HT2A receptors antagonist M100907 prevents impairment in attentional performance by NMDA receptor blockade in the rat prefrontal cortex. *Neuropsychopharmacology* **29**:1637–1647.

Moghaddam B, Adams B, Verma A, and Daly D (1997) Activation of glutamatergic neurotransmission by ketamine: a novel step in the pathway from NMDA receptor blockade to dopaminergic and cognitive disruptions associated with the prefrontal cortex. *J Neurosci* **17**:2921–2927.

Morgan CJ, Mofeez A, Brandner B, Bromley L, and Curran HV (2004) Acute effects of ketamine on memory systems and psychotic symptoms in healthy volunteers. *Neuropsychopharmacology* **29**:208–218.

Nyberg S, Eriksson B, Oxenstierna G, Halldin C, and Farde L (1999) Suggested minimal effective dose of risperidone based on PET-measured D2 and 5-HT2A receptor occupancy in schizophrenic patients. *Am J Psychiatry* **156**:869–875.

Oranje B, Gispen-de Wied CC, Westenberg HG, Kemner C, Verbaten MN, and Kahn RS (2009) Haloperidol counteracts the ketamine-induced disruption of processing negativity, but not that of the P300 amplitude. *Int J Neuropsychopharmacol* **12**: 823–832.

Rasmussen CE, Williams CKI (2006) *Gaussian Processes for Machine Learning*, MIT Press, Cambridge, MA.

Schmidt CJ and Fadayel GM (1996) Regional effects of MK-801 on dopamine release: effects of competitive NMDA or 5-HT2A receptor blockade. *J Pharmacol Exp Ther* **277**:1541–1549.

Stone JM, Dietrich C, Edden R, Mehta MA, De Simoni S, Reed LJ, Krystal JH, Nutt D, and Barker GJ (2012) Ketamine effects on brain GABA and glutamate levels with 1H-MRS: relationship to ketamine-induced psychopathology. *Mol Psychiatry* **17**:664–665.

Tauscher J, Hussain T, Agid O, Verhoeff NPLG, Wilson AA, Houle S, Remington G, Zipursky RB, and Kapur S (2004) Equivalent occupancy of dopamine D1 and D2 receptors with clozapine: differentiation from other atypical antipsychotics. *Am J Psychiatry* **161**:1620–1625.

Varnäs K, Halldin C, and Hall H (2004) Autoradiographic distribution of serotonin transporters and receptor subtypes in human brain. *Hum Brain Mapp* **22**:246–260.

Varty GB, Bakshi VP, and Geyer MA (1999) M100907, a serotonin 5-HT2A receptor antagonist and putative antipsychotic, blocks dizocilpine-induced prepulse inhibition deficits in Sprague-Dawley and Wistar rats. *Neuropsychopharmacology* **20**:311–321.

Vollenweider FX, Leenders KL, Scharfetter C, Antonini A, Maguire P, Missimer J, and Angst J (1997) Metabolic hyperfrontality and psychopathology in the ketamine model of psychosis using positron emission tomography (PET) and [18F]fluorodeoxyglucose (FDG). *Eur Neuropsychopharmacol* **7**:9–24.

Wong EC, Buxton RB, and Frank LR (1997) Implementation of quantitative perfusion imaging techniques for functional brain mapping using pulsed arterial spin labeling. *NMR Biomed* **10**:237–249.

**Address correspondence to:** Orla M. Doyle. Department of Neuroimaging, Institute of Psychiatry (PO89), De Crespigny Park, London SE5 8AF, UK. E-mail: orla.doyle@kcl.ac.uk